Transonic Canards and Stellar Wind

Paul Carter* Edgar Knobloch† Martin Wechselberger‡

January 6, 2017

Abstract

Parker's classical stellar wind solution [20] describing steady spherically symmetric outflow from the surface of a star is revisited. Viscous dissipation is retained. The resulting system of equations has slow-fast structure and is amenable to analysis using geometric singular perturbation theory. This technique leads to a reinterpretation of the sonic point as a folded saddle and the identification of shock solutions as canard trajectories in space [22]. The results shed light on the location of the shock and its sensitivity to the system parameters. The related spherically symmetric stellar accretion solution of Bondi [4] is described by the same theory.

keywords: transonic flow, stellar wind, canards, geometric singular perturbation theory

1 Introduction

Most material in the universe is in gaseous form. On average, a gas particle will travel a certain distance, the *mean free path*, before changing its state of motion by colliding with another particle. Provided we are interested only in length scales that are significantly larger than the mean free path, we can regard the gas as a continuous fluid and its properties are then described by the equations of gas dynamics. This paper concerns *transonic* flows, i.e., gas flows exhibiting transitions between subsonic and supersonic flow, arising in the theory of stellar accretion and stellar wind theory. We analyse the mathematical properties of steady radial flows of either type from a geometric singular perturbation theory (GSPT) point of view [5], focusing on viscous stationary spherically symmetric transonic flows, and provide geometric interpretations of the classical stellar wind solution of Parker [20] and the related spherically symmetric stellar accretion solution of Bondi [4] in the context of *canard theory* [3, 22, 23].

We study the flow of a viscous compressible fluid (gas) described by the equations (see, e.g., [17])

$$\begin{aligned} &\rho_t + \nabla\cdot(\rho u) = 0, \\ &(\rho u)_t + \nabla\cdot(\rho(uu) + pI) - F = \eta_1 \nabla\cdot(\nabla u + (\nabla u)^T) + \eta_2 \nabla\cdot((\nabla\cdot u)I), \end{aligned} \tag{1.1}$$

*Department of Mathematics, University of Arizona, Tucson, AZ 85721, USA

†Department of Physics, University of California at Berkeley, Berkeley, CA 94720, USA

‡School of Mathematics & Statistics, University of Sydney, Sydney, NSW 2006, Australia (corresponding author)

where $\rho > 0$ is the density of the fluid, $u \in \mathbb{R}^3$ is the Eulerian velocity of the fluid, F is the external (gravitational) force and $p > 0$ is the thermodynamic pressure. The first equation describes the continuity equation (conservation of mass) and the second is Euler's equation (conservation of momentum). The quantity $\eta_1 = \eta_{shear}$ is the shear viscosity (dynamic viscosity) while $\eta_2 := \eta_{bulk} - 2/3\,\eta_{shear}$ is a combination of the shear and bulk viscosities of the fluid; in the following both will be assumed to be constants, independent of position. Viscous effects are important in flows which show either large shearing motion or steep velocity gradients (shocks).

Assumption 1.1. *In the absence of viscous effects the entropy of a comoving fluid element is constant (ideal fluid). The pressure $p(\rho)$ is a function of the density ρ which satisfies*

$$p(\rho) = \beta \rho^\gamma, \tag{1.2}$$

where the adiabatic index γ, assumed to be constant, satisfies $1 \leq \gamma \leq 5/3$. The parameter $\beta \equiv p\rho^{-\gamma} > 0$ is constant independent of the streamline, i.e., we consider an isentropic flow. The two extreme cases of interest are isothermal flow *(constant temperature) corresponding to $\gamma = 1$ and* adiabatic flow *corresponding to $\gamma = 5/3$ (monoatomic gas).*

Remark 1.1. *Formula* (1.2) *replaces the energy equation for the fluid (the third conservation equation of fluid dynamics).*

Assumption 1.2. *The only external force we assume to be acting is gravity, i.e.,*

$$F = -\rho g \tag{1.3}$$

where g is the local acceleration due to gravity.

Remark 1.2. *We assume the gas is unmagnetised and ignore all magnetic field effects.*

System (1.1) under Assumptions 1.1 and 1.2 defines the astrophysical flow problem we analyse in the following.

1.1 Steady, spherically symmetric viscous gas flow

We consider a star of mass M, at rest in an infinite gas cloud which is itself at rest at infinity and of uniform density ρ_∞ and pressure p_∞ at infinity. We are interested in spherically symmetric solutions of (1.1) which are functions of (r, t) only and satisfy the following system:

$$\begin{gathered}
\rho_t + \frac{1}{r^2}\frac{\partial}{\partial r}(\rho r^2 u) = 0, \\
(\rho u)_t + \frac{1}{r^2}\frac{\partial}{\partial r}(\rho r^2 u^2) + \frac{\partial p}{\partial r} + \rho\frac{GM}{r^2} = \eta\frac{\partial}{\partial r}\left(\frac{1}{r^2}\frac{\partial}{\partial r}(r^2 u)\right),
\end{gathered} \tag{1.4}$$

where $\eta := 2\eta_1 + \eta_2 = \eta_{bulk} + 4/3\,\eta_{shear} \geq 0$ is the resulting combined viscosity (see, e.g. [17]), and the gravitational force has only a radial component, i.e.,

$$F = -\rho \frac{GM}{r^2} \hat{r}$$

with $G > 0$ as the gravitational constant. Note that $u \in \mathbb{R}$ is now the radial velocity, where $u < 0$ corresponds to inflow (towards the star) and $u > 0$ to outflow (away from the star). The flow is *supersonic* if $|u| > c$ and *subsonic* if $|u| < c$, where

$$c = \left(\frac{dp}{d\rho}\right)^{1/2} > 0 \tag{1.5}$$

denotes the adiabatic speed of sound. Note that c is independent of r only in the isothermal case $\gamma = 1$ and is then equal to $\sqrt{\beta}$.

For steady flow, Eqs. (1.4) reduce to the ordinary differential equations

$$\begin{aligned} \frac{1}{r^2}\frac{d}{dr}(\rho r^2 u) &= 0, \\ \frac{1}{r^2}\frac{d}{dr}(\rho r^2 u^2) + \frac{dp}{dr} + \rho\frac{GM}{r^2} &= \eta \frac{d}{dr}\left(\frac{1}{r^2}\frac{d}{dr}(r^2 u)\right). \end{aligned} \tag{1.6}$$

The continuity equation implies $\rho r^2 u = K$ with constant *mass flux* $|K|$, i.e., for inflow ($u < 0$) we have $K < 0$ while for outflow ($u > 0$) we have $K > 0$. We can solve this equation to obtain the density as a function of the radial distance r and the velocity u,

$$\rho = \rho(u, r) = \frac{K}{r^2 u} > 0\,, \tag{1.7}$$

and hence obtain the pressure $p = p(\rho(u, r))$ through (1.2). We are left with the (viscous) Euler equation

$$\frac{1}{r^2}\frac{d}{dr}(\rho r^2 u^2) + \frac{dp}{dr} + \rho\frac{GM}{r^2} = \eta \frac{d}{dr}\left(\frac{1}{r^2}\frac{d}{dr}(r^2 u)\right) \tag{1.8}$$

to determine the velocity $u = u(r)$. This equation can be rewritten in the form

$$\frac{d}{dr}\underbrace{\left(p + \rho u^2 - \eta\frac{du}{dr} - \eta\frac{2u}{r}\right)}_{:=m} = -\frac{2\rho u^2}{r} - \rho\frac{GM}{r^2}\,. \tag{1.9}$$

We therefore define the auxiliary variable

$$m := p + \rho u^2 - \eta\frac{du}{dr} - \eta\frac{2u}{r}\,, \tag{1.10}$$

leading to the following system of first order nonautonomous ordinary differential equations:

$$\begin{aligned} \frac{dm}{dr} &= -\frac{2\rho u^2}{r} - \rho\frac{GM}{r^2} \\ \eta\frac{du}{dr} &= -m + \rho u^2 + p - \eta\frac{2u}{r}\,. \end{aligned} \tag{1.11}$$

Remark 1.3. *The auxiliary variable m is a pressure-like variable, equal to the sum of the thermodynamic pressure p and the ram pressure ρu^2 when viscosity is neglected (cf. [25], Ch. 6). As shown below an important property of this variable is that it remains continuous across shocks even in the inviscid limit $\eta \to 0$ while the velocity u, thermodynamic pressure p and density ρ all develop discontinuities.*

1.2 Statement of main result: stellar wind/accretion solutions

Equations (1.11) are to be solved subject to appropriate (astro)physical boundary conditions. We consider an infinite gas cloud at rest as $r \to \infty$ with uniform density $\rho \to \rho_\infty > 0$ and pressure $p \to p_\infty > 0$. This defines the ambient boundary condition $m \to m_\infty = p_\infty$ for (1.11). A second condition is given by fixing the mass flux $|K|$ which is equivalent of fixing $\rho(r_0)u(r_0) = \rho_0 u_0$ at a location $r = r_0 > 0$ near the stellar surface[1] through (1.7). With this astrophysically motivated choice of the inner boundary, we avoid the singularity at $r = 0$ in (1.11), even though this singularity can be handled mathematically. We note that the density $\rho(r)$ (equivalently, velocity $u(r)$) is not fixed by these boundary conditions, although the constant mass flux $|K|$ in (1.7) with $\rho_\infty > 0$ demands that the speed u decays as $1/r^2$ as $r \to \infty$. We also assume that the speed u_0 at the stellar surface is subsonic, i.e. $u_0 < c(r_0) := c_0$. Thus the specification of r_0, K and m_∞ suffices to determine a transonic solution of (1.11).

Since $u(r_1) := u_1$ must be subsonic for sufficiently large r_1 we can restrict our analysis to a bounded domain $r \in [r_0, r_1]$. From a mathematical point of view, we simply shift the ambient boundary condition $p \to p_\infty$ to $p(r_1) := p_1$ at $r = r_1$, assuming that p_1 corresponds to the original boundary condition $p \to p_\infty$.[2] Moreover, the use of a bounded domain enables us to compare our results directly with numerical solutions of the partial differential equations (PDEs) (1.4).

Our aim is thus to find transonic solutions such that u_0 is subsonic at $r = r_0$ but u becomes supersonic at some $r = r_c > r_0$ (see [8], sections 2 and 3) before it becomes subsonic again at $r = r_j > r_c$, $r_j < r_1$. In the outflow problem, these are the *stellar wind* solutions, and for the inflow problem, these are the transonic *accretion* solutions.

Definition 1.1. *A* transonic *solution $(m, u) = (m(r), u(r))$ to (1.11) fulfills:*

(i) $|u(r_0)|$ and $|u(r_1)|$ are subsonic at the boundaries.

(ii) $|u(r)|$ is supersonic for $r \in I_{super}$, where $I_{super} \subset (r_0, r_1)$ is a closed interval.

If $u > 0$ for all r, then we refer to (m, u) as a transonic stellar wind solution*; if $u < 0$ for all r, then we refer to (m, u) as a* transonic stellar accretion solution.

With this definition, we have the following theorem, which is the main result of this paper.

[1] The solar wind is in fact accelerated through energy deposition into the flow above the surface of the Sun and it is this process that is ultimately responsible for specifying K. However, in the following we take K to be prescribed and refer to $r = r_0$ as the stellar surface.

[2] In principle p_1 can be calculated through compactification.

Theorem 1.1. *Given* (1.4), *respectively* (1.11), *with fixed* $\gamma \in [1, 5/3)$, *mass flux* $|K| > 0$ *and sufficiently large Reynolds number* $Re \gg 1$ *the following statements hold.*

(i) For the outflow problem $u > 0$, *there exists an open pressure interval* (p_1^c, p_1^f) *such that for a given ambient pressure* $p(r_1) = p_1 \in (p_1^c, p_1^f)$, *there exists a pressure* $p^c(r_0) = p_0^c$ *at the stellar surface* $r = r_0$ *that supports a steady transonic stellar wind solution with these boundary conditions.*

(ii) For the inflow problem $u < 0$, *there exists an open pressure interval* (p_0^c, p_0^f) *such that for a given surface pressure* $p(r_0) = p_0 \in (p_0^c, p_0^f)$, *there exists an ambient pressure* $p^c(r_1) = p_1^c$ *that supports a steady transonic stellar accretion solution with these boundary conditions.*

If $\gamma = 5/3$, *then no transonic solutions exist.*

Remark 1.4. *The assumption of large Reynolds number* $Re \gg 1$, *i.e. that inertial forces dominate viscous forces, is a natural assumption in this type of system.*

In the outflow problem $u > 0$, *the mass flux* $|K|$ *determines the surface pressure* p_0 *that leads to a transonic solution. This solution must undergo a reverse transition to subsonic flow in order to connect to the ambient pressure* p_1 *at* r_1. *When* $Re \gg 1$, *this transition takes the form of a 'shock' whose position is determined by* p_1.

Similarly, for the inflow problem $u < 0$, *the mass flux* $|K|$ *determines the pressure* p_1 *that leads to a transonic solution. This solution must undergo a reverse transition to subsonic flow in order to connect to the pressure* p_0 *at the stellar surface* r_0. *When* $Re \gg 1$, *this transition takes the form of a 'shock' whose position is determined by* p_0.

Remark 1.5. *We discuss briefly the intervals of admissible boundary pressure values in Theorem 1.1:*

For the outflow problem $u > 0$, *if the ambient pressure is too strong, i.e.* $p_1 > p_1^f$, *then there still exists a* p_0 *that supports a steady solution, but this solution is entirely subsonic. Solutions of this type are known as stellar breezes. If the ambient pressure is too weak, i.e.* $p_1 < p_1^c$, *then no steady solution is supported with subsonic speed* u_0 *at* $r = r_0$ *within this model.*

Similarly, for the inflow problem $u < 0$, *if the surface pressure is too strong, i.e.* $p_0 > p_0^f$, *then there still exists a* p_1 *that supports a steady solution, but this solution is entirely subsonic. If the star pressure is too weak, i.e.* $p_0 < p_0^c$, *then no steady solution is supported with subsonic speed* u_1 *at* $r = r_1$ *within this model.*

Remark 1.6. *For* $\eta > 0$, *we solve* (1.11) *as a nonlinear two-point boundary value problem with a condition on the pressure, say, imposed at* $r = r_0$ *and again at* $r = r_1$. *This problem has a unique smooth solution only for discrete values of a nonlinear eigenvalue (for example, the flux* K*). Since* K *is determined in practice by acceleration near the stellar surface we instead adjust the location of the far boundary to the assumed value of* K. *In either case as* $\eta \to 0$ *this solution sharpens and forms a shock, and very small adjustments in the boundary conditions and/or location suffice to account for the effects of finite* η *when* η *is small.*

The remainder of this paper is laid out as follows. In section 2, we perform a dimensional analysis which identifies (1.11) as a singular perturbation problem. In section 3, we describe the geometric singular perturbation approach that takes advantage of the slow fast splitting of variables and, in particular, provides a geometric interpretation of the *sonic point* and *shock* conditions. This allows us in section 4 to construct the corresponding transonic solutions outlined in Definition 1.1, and to prove their existence as stated in Theorem 1.1. Section 5 contains a brief numerical study, followed by a discussion of the results in section 6.

2 Dimensional analysis

The first step in our analysis is to nondimensionalize (1.11). Only then can we understand the relative sizes of the terms involved and hence the structure of the equations. The following table shows the variables, parameters and their scales using SI units:

	Name	SI unit
u	velocity	m/s
m	total pressure	$kg/(m \cdot s^2)$
r	radial distance	m
ρ	density	kg/m^3
p	thermodynamic pressure	$kg/(m \cdot s^2)$
G	gravitational constant	$m^3/(kg \cdot s^2)$
M	(point) mass of stellar object	kg
η	viscosity	$kg/(m \cdot s)$
γ	adiabatic index	1
$\lvert K\rvert$	mass flux	kg/s
β	entropy parameter	$(m/s)^2 \cdot (kg/m^3)^{1-\gamma}$

It is convenient to introduce natural reference scales for the dependent and independent variables under study, here (u, m, r). In the context of astrophysical gas dynamics, a natural reference velocity is the adiabatic speed of sound (1.5),

$$c = \left(\frac{dp}{d\rho}\right)^{1/2} = (\gamma\beta)^{\frac{1}{2}} \left(\frac{K}{r^2 u}\right)^{\frac{\gamma-1}{2}} > 0\,. \tag{2.1}$$

To cover all possible values of the adiabatic index γ, we introduce the local *Mach number* v of the flow defined by

$$u = cv,$$

and rewrite the system (1.11) in the form

$$\begin{aligned} \frac{dm}{dr} &= -\frac{2\rho}{r}\left(c^2v^2 + \frac{GM}{2r}\right) \\ \eta\frac{dv}{dr} &= \left(\frac{\gamma+1}{2}\right)\frac{1}{c}\left(-m + \rho c^2 v^2 + p\right) - 2\eta\frac{v}{r}\,. \end{aligned} \tag{2.2}$$

Here we used the fact that

$$\frac{dc}{dr} = -\left(\frac{\gamma-1}{2}\right) c \left(\frac{2}{r} + \frac{1}{u}\frac{du}{dr}\right).$$

Next we introduce dimensionless variables n and s through

$$m = k_m n\,, \qquad r = k_r s\,,$$

with reference scales k_m and k_r (yet to be determined), yielding the dimensionless nonautonomous system

$$\begin{aligned} \frac{dn}{ds} &= -\frac{2\bar\rho}{s}\left(\frac{k_\rho k_c^2}{k_m}\bar c^2 v^2 + \frac{GMk_\rho}{2k_m k_r}\frac{1}{s}\right) \\ \frac{\eta k_c}{k_m k_r}\frac{dv}{ds} &= \left(\frac{\gamma+1}{2}\right)\frac{1}{\bar c}\left(-n + \frac{k_\rho k_c^2}{k_m}\bar\rho \bar c^2 v^2 + \frac{k_p}{k_m}\bar p\right) - \frac{\eta k_c}{k_m k_r}\frac{2v}{s}\,. \end{aligned} \tag{2.3}$$

Here

$$c = k_c \bar c\,, \quad \rho = k_\rho \bar\rho\,, \quad p = k_p \bar p\,,$$

and $(\bar c, \bar\rho, \bar p)$ represent the dimensionless (adiabatic) speed of sound, density and thermodynamic pressure, respectively, given by the expressions

$$\bar c = \left(\frac{1}{s^2|v|}\right)^{\frac{\gamma-1}{\gamma+1}}\,, \quad \bar\rho = \left(\frac{1}{s^2|v|}\right)^{\frac{2}{\gamma+1}}\,, \quad \bar p = \frac{1}{\gamma}\left(\frac{1}{s^2|v|}\right)^{\frac{2\gamma}{\gamma+1}} = \frac{1}{\gamma}\,\bar\rho^\gamma\,, \tag{2.4}$$

with (derived) reference scales

$$k_c = (\gamma\beta)^{\frac{1}{\gamma+1}}\left(\frac{|K|}{k_r^2}\right)^{\frac{\gamma-1}{\gamma+1}}\,, \quad k_\rho = (\gamma\beta)^{-\frac{1}{\gamma+1}}\left(\frac{|K|}{k_r^2}\right)^{\frac{2}{\gamma+1}}\,, \quad k_p = (\gamma\beta)^{\frac{1}{\gamma+1}}\left(\frac{|K|}{k_r^2}\right)^{\frac{2\gamma}{\gamma+1}}\,.$$

Note that $\bar c^2 = \bar p_{\bar\rho}$, i.e., we have the equivalent dimensionless definition of the adiabatic speed of sound. By choosing[3]

$$k_m := k_p\,,$$

where $k_p = k_\rho k_c^2$, we obtain the dimensionless nonautonomous system

$$\begin{aligned} \frac{dn}{ds} &= -\frac{2\bar\rho}{s}\left(\bar c^2 v^2 + \frac{\alpha}{s}\right) \\ \varepsilon\frac{dv}{ds} &= \left(\frac{\gamma+1}{2}\right)\frac{1}{\bar c}\left(-n + \bar\rho\bar c^2 v^2 + \bar p\right) - \varepsilon\frac{2v}{s} \end{aligned} \tag{2.5}$$

parametrized, in addition to γ, by the two dimensionless parameters

$$\alpha := \frac{GM}{2k_r k_c^2} = \frac{GM}{2}(\gamma\beta)^{-\frac{2}{\gamma+1}}|K|^{\frac{2(1-\gamma)}{\gamma+1}} k_r^{\frac{3\gamma-5}{\gamma+1}}\,, \tag{2.6}$$

$$\varepsilon := \frac{\eta}{k_r k_\rho k_c} = \frac{\eta k_r}{|K|}\,. \tag{2.7}$$

[3]Recall from Remark 1.3 that m is a pressure-like variable.

Note the reduction from five dimensional parameters $(G, M, \eta, |K|, \beta)$ to two dimensionless parameters (α, ε) as expected from dimensional analysis. By choosing

$$k_r := \left[\left(\frac{GM}{2} \right)^{\gamma+1} (\gamma\beta)^{-2} |K|^{2(1-\gamma)} \right]^{\frac{1}{5-3\gamma}}, \tag{2.8}$$

a quantity defined for $1 \leq \gamma < 5/3$ only, we can fix the dimensionless parameter $\alpha = 1$ defined in (2.6). Note that the length scale k_r defined in (2.8) depends sensitively on γ in the limit $\gamma \to 5/3$.

Assumption 2.1. *Let* $u_{\mathrm{esc}} := \sqrt{2GM/r_0}$ *be the* escape speed *from the surface of the star. We require that* $u_{\mathrm{esc}} > 2c_0$*, where* $c_0 = c(r_0)$ *denotes the adiabatic speed of sound at the stellar surface.*

Lamers and Cassinelli [16] show that in the isothermal case $u_{\mathrm{esc}} > 2c_0$; their Table 3.1 provides a comparison between the escape speed and the isothermal sound speed. This observation remains valid for the polytropic case for any $1 < \gamma \leq 5/3$.

With p_0, ρ_0 denoting the pressure and density at the stellar surface, the corresponding adiabatic sound speed (Eq. (2.1)) is $c_0 = \sqrt{\gamma p_0/\rho_0}$. Using $\beta = p_0 \rho_0^{-\gamma}$ (Assumption 1.1) and the fact that $|K| = \rho_0 r_0^2 |u_0|$ (Eq. (1.7)) allows us to factorize (2.8) as follows:

$$k_r = \left[\left(\frac{u_{\mathrm{esc}}}{2c_0} \right)^{\gamma+1} \left(\frac{c_0}{|u_0|} \right)^{\gamma-1} \right]^{\frac{2}{5-3\gamma}} r_0 =: \sigma_0 r_0 \,, \tag{2.9}$$

where u_0 is the speed at $r = r_0$. Since $\dfrac{2}{5-3\gamma} \geq 1$ for $1 \leq \gamma < 5/3$ we see that $\sigma_0 > 1$ whenever

$$\frac{|u_0|}{c_0} < \left(\frac{u_{\mathrm{esc}}}{2c_0} \right)^{\frac{\gamma+1}{\gamma-1}} . \tag{2.10}$$

Based on Assumption 2.1 it follows that the condition $\sigma_0 > 1$ holds for all winds that are subsonic at the stellar surface. For such winds $k_r > r_0$.

The inverse of the dimensionless parameter ε (2.7) represents the *Reynolds number* *Re* of the flow at the stellar surface:

$$\frac{1}{\varepsilon} = \frac{k_r k_\rho k_c}{\eta} = \frac{\text{inertial forces}}{\text{viscous forces}} =: Re \,.$$

As in (2.9), we are able to factorize ε:

$$\varepsilon = \sigma_0 \frac{\eta_0}{\rho_0 r_0 |u_0|} =: \sigma_0 \varepsilon_0 \,. \tag{2.11}$$

Thus the order of magnitude of ε is determined by ε_0 for $1 \leq \gamma < 5/3$. We estimate ε_0 using typical parameter values for conditions near the solar surface [19]. For ionized hydrogen $\eta_0 \approx 1.2 \times 10^{-16} T_0^{5/2}\, g\, cm^{-1}\, s^{-1}$, $\rho_0 = 3 \times 10^7 m_H\, g\, cm^{-3}$, where m_H is the mass of a proton in grams, and $r_0 = 10^{11}\,cm$. Assuming a typical outflow velocity $u_0 \sim 2\times 10^7\,cm\,s^{-1}$ and surface temperature $T_0 = 10^4\,{}^\circ$K, we obtain the estimate $\epsilon_0 \approx 10^{-8}$; if the temperature of the corona is used instead the estimate becomes $\epsilon_0 \approx 10^{-3}$. Thus the conclusion that $\varepsilon_0 \ll 1$ is robust despite the rapidly changing conditions in this region and inertial forces dominate viscous forces throughout the flow whenever γ is bounded away from $\gamma = 5/3$ – unless there are regions in which gradients are locally very large. Such regions are associated with the presence of *shocks*.

To deal with the $\gamma = 5/3$ case we have to choose a different characteristic length scale. We use the radius r_0 of the star,

$$k_r := r_0\,, \tag{2.12}$$

i.e., we take $\sigma_0 = k_r/r_0 = 1$. In fact this choice works for all $\gamma \in [1, 5/3]$ but α is then no longer unity:

$$\alpha = \left(\frac{u_{\text{esc}}}{2c_0}\right)^2 \left(\frac{c_0}{|u_0|}\right)^{\frac{2(\gamma-1)}{\gamma+1}}\,. \tag{2.13}$$

From Assumption 2.1 it follows that $\alpha > 1$ for all winds that are subsonic at the stellar surface. Moreover

$$\varepsilon = \varepsilon_0 = \frac{\eta_0}{\rho_0 r_0 |u_0|} \ll 1\,, \tag{2.14}$$

as shown before.

We perform our analysis first with k_r defined by (2.8) and then explain how the results relate to the case where the scale (2.12) is used instead. We consider (2.5) as a singularly perturbed system with singular perturbation parameter $\varepsilon \ll 1$ for all $\gamma \in [1, 5/3]$ recalling the different definitions of k_r where necessary, and study its solutions subject to Dirichlet boundary conditions on (n, v) at $s_0 \equiv r_0/k_r$, respectively $s_1 \equiv r_1/k_r$, implied by the choice of (2.9), respectively (2.12).

We give the equivalent definition of a transonic solution:

Definition 2.1. *A* transonic *solution* $(n, v) = (n(s), v(s))$ *to* (2.5) *fulfills:*

(i) $|v(s_0)| < 1$ *and* $|v(s_1)| < 1$ *at the boundaries.*

(ii) $|v(s)| > 1$ *for* $s \in I_{super}$*, where* $I_{super} \subset (s_0, s_1)$ *is a closed interval.*

If $v > 0$ *for all* s*, then we refer to* (n, v) *as a* transonic stellar wind solution*; if* $v < 0$ *for all* s*, then we refer to* (n, v) *as a* transonic stellar accretion solution.

With this definition, we can reformulate Theorem 1.1 in terms of dimensionless variables. Given the relations (2.4), at the fixed values of $s = s_0, s_1$, the pressure boundary conditions from Theorem 1.1 may be equivalently expressed in terms of the Mach number v.

Theorem 2.1. *Consider* (2.5) *with fixed* $\gamma \in [1, 5/3)$ *and* $s_0 < 1 < s_1$*. We have the following.*

(i) For the outflow problem $v > 0$, there exist $0 < v_1^f < v_1^c < 1$ such that for each $v_1 \in (v_1^f, v_1^c)$ and each sufficiently small $\epsilon > 0$, there exists $v_0^c = v_0^c(\epsilon) \in (0,1)$ and a steady transonic stellar wind solution satisfying $v(s_0) = v_0^c(\epsilon)$ and $v(s_1) = v_1$. For $0 < v_1 < v_1^f$, there exists a solution to (2.5), but it is entirely subsonic, and for $v_1 > v_1^c$, there is no solution which is subsonic at $s = s_0$.

(ii) For the inflow problem $v < 0$, there exist $-1 < v_0^c < v_0^f < 0$ such that for each $v_0 \in (v_0^c, v_0^f)$ and each sufficiently small $\epsilon > 0$, there exists $v_1^c = v_1^c(\epsilon) \in (-1,0)$ and a steady transonic stellar accretion solution satisfying $v(s_0) = v_0$ and $v(s_1) = v_1^c(\epsilon)$. For $v_0^f < v_0 < 0$, there exists a solution to (2.5), but it is entirely subsonic, and for $v_0 < v_0^c$, there is no solution which is subsonic at $s = s_1$.

If $\gamma = 5/3$, then no transonic solutions exist.

3 Geometric singular perturbation approach

First, we introduce a dummy *slow* variable $dy := \pm ds$ in the system (2.5), where the positive sign refers to the outflow ($v > 0$) problem and the minus sign to the inflow ($v < 0$) problem, and write

$$\begin{aligned}
\frac{ds}{dy} &= \pm 1 =: g_1(s,n,v,\varepsilon)\\
\frac{dn}{dy} &= \mp\frac{2\bar{\rho}}{s}\left(\bar{c}^2v^2 + \frac{\alpha}{s}\right) =: g_2(s,n,v,\varepsilon)\\
\varepsilon\frac{dv}{dy} &= \pm\left(\frac{\gamma+1}{2}\right)\frac{1}{\bar{c}}\left(-n + \bar{\rho}\bar{c}^2v^2 + \bar{p}\right) \mp \varepsilon\frac{2v}{s} =: f(s,n,v,\varepsilon)\,,
\end{aligned} \tag{3.1}$$

yielding an autonomous singularly perturbed system with 'slow' variables (s,n), 'fast' variable v and a singular perturbation parameter $\varepsilon \ll 1$.

Remark 3.1. *Recall that we can set $\alpha = 1$ for all $\gamma \in [1, 5/3)$.*

While this system is now autonomous and hence suitable for a classic geometric singular perturbation analysis [5, 13, 24], it has no equilibria as expected from a nonautonomous system.

By rescaling the independent dummy variable $y = \varepsilon z$, we obtain the equivalent singularly perturbed system

$$\begin{aligned}
\frac{ds}{dz} &= \varepsilon g_1(s,n,v,\varepsilon)\\
\frac{dn}{dz} &= \varepsilon g_2(s,n,v,\varepsilon)\\
\frac{dv}{dz} &= f(s,n,v,\varepsilon)
\end{aligned} \tag{3.2}$$

evolving on the *fast* scale z. The singular nature of these systems is revealed by taking the limit $\varepsilon \to 0$. For the fast system (3.2) this yields the *layer problem*

$$\begin{aligned}
\frac{ds}{dz} &= 0 \\
\frac{dn}{dz} &= 0 \\
\frac{dv}{dz} &= \pm\left(\frac{\gamma+1}{2}\right)\frac{1}{\bar{c}}\left(-n+\bar{\rho}\bar{c}^2v^2+\bar{p}\right) = f(s,n,v,0)
\end{aligned} \tag{3.3}$$

for the evolution of the fast variable v. Note that the slow variables (s,n) are parameters in the layer problem. Hence this is a one-dimensional problem where the slow variables are bifurcation parameters.

On the other hand, for the slow system (3.1) the result of taking the limit $\varepsilon \to 0$ is the *reduced problem*

$$\begin{aligned}
\frac{ds}{dy} &= \pm 1 = g_1(s,n,u,0) \\
\frac{dn}{dy} &= \mp\frac{2\bar{\rho}}{s}\left(\bar{c}^2v^2+\frac{\alpha}{s}\right) = g_2(s,n,v,0) \\
0 &= \pm\left(\frac{\gamma+1}{2}\right)\frac{1}{\bar{c}}\left(-n+\bar{\rho}\bar{c}^2v^2+\bar{p}\right) = f(s,n,v,0)\,,
\end{aligned} \tag{3.4}$$

which is a two-dimensional differential-algebraic system for the evolution of the slow variables (s,n). The phase space of the reduced problem is defined by the algebraic constraint $0 = f(s,n,v,0)$ and is called the *critical manifold*:

$$S := \{(s,n,v) \in \mathbb{R}^3 \,:\, f(s,n,v,0) = 0\}\,.$$

It is also the equilibrium manifold of the layer problem (3.3) and plays a key role in understanding the dynamics of the singularly perturbed problem under study.

The main idea of geometric singular perturbation theory [5, 13] is to concatenate solutions of the two limiting lower dimensional problems (3.3) and (3.4) to obtain an approximate solution of the full problem (3.2), resp. (3.1), and then show that such a solution will persist under small perturbations $\varepsilon \ll 1$.

3.1 Layer problem

System (3.3) evolves along one-dimensional fast fibers $(n,s) =$ constant in three-dimensional phase space. Here, the critical manifold S is a two-dimensional manifold of equilibria. Observing that

$$\frac{\partial f}{\partial n} := f_n = \mp\left(\frac{\gamma+1}{2}\right)\frac{1}{\bar{c}} \lesseqgtr 0$$

and

$$\frac{\partial f}{\partial s} := f_s = \mp 2\frac{\overline{\rho c}}{s}(\gamma v^2+1) \lesseqgtr 0$$

evaluated along the critical manifold S, the *implicit function theorem (IFT)* implies that $f = 0$ can be solved (locally) for n (or s). Here, S has a graph representation which we can give explicitly:

$$S = \{(s, n, v) \in \mathbb{R}^3 \,:\, n = N(s, v)\},$$

where

$$N(s, v) := \bar{\rho}\bar{c}^2 v^2 + \bar{p} = \gamma\bar{p}\left(v^2 + \frac{1}{\gamma}\right) = \bar{\rho}^\gamma\left(v^2 + \frac{1}{\gamma}\right).$$

We have the following.

Proposition 3.1. *The critical manifold $S = S_a \cup F \cup S_r$ is folded with an attracting subsonic branch S_a, sonic fold curve F and a repelling supersonic branch S_r.*

Proof. We investigate the stability properties along S, i.e., we calculate the Jacobian in the fast direction which is simply the partial derivative of f with respect to the fast variable v,

$$\frac{\partial f}{\partial v} = f_v = \pm\frac{\bar{\rho}\bar{c}}{v}(v^2 - 1)\,, \tag{3.5}$$

where we have used the fact that

$$\bar{\rho}_v = -\left(\frac{2}{\gamma + 1}\right)\frac{\bar{\rho}}{v}\,, \qquad \bar{c}^2\bar{\rho} = \gamma\bar{p}\,.$$

Since $v^2 = 1$ corresponds to locations where the flow speed equals the sound speed (Mach number = 1), we obtain the following stability result for the critical manifold S:

$$\left.\begin{matrix} f_v < 0 \\ f_v = 0 \\ f_v > 0 \end{matrix}\right\} \text{ for } \begin{cases} 1 > v^2 & \text{subsonic, attracting} \\ 1 = v^2 & \text{sonic} \\ 1 < v^2 & \text{supersonic, repelling.} \end{cases}$$

Next, we observe that

$$f_{vv} = \pm\bar{\rho}\bar{c}\left(1 + \frac{1}{v^2}\right) \gtrless 0$$

evaluated along the sonic curve $v^2 = 1$, which we denote by F. Hence $S = S_a \cup F \cup S_r$ is folded along the sonic curve, with attracting branch S_a ($v^2 < 1$) and repelling branch S_r ($v^2 > 1$). □

Note that the Jacobian of $\{f = 0, f_v = 0\}$ evaluated along the fold F is given by

$$J = \begin{pmatrix} f_s & f_n & 0 \\ f_{vs} & f_{vn} & f_{vv} \end{pmatrix}. \tag{3.6}$$

Thus the IFT implies that the sonic fold curve F can be parametrized (locally) by s, i.e.,

$$F = \{(s, n, v) \in S \,:\, n = N(s, V(s)), v = V(s) = \pm 1,\, s > 0\}\,.$$

An example of the folded critical manifold is shown in Figure 1 for $\gamma = 7/5$. The fold structure (i.e. the sonic curve) is clearly visible.

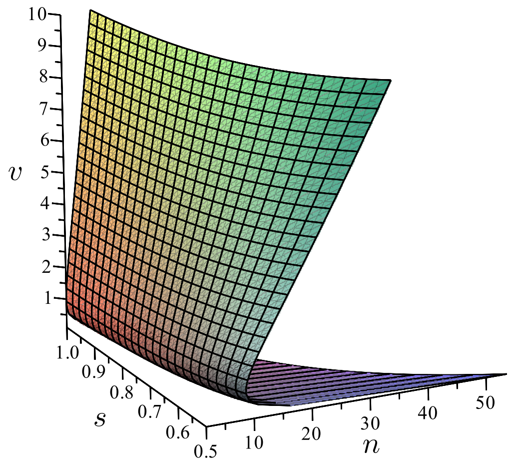

Figure 1: Folded critical manifold S for $\gamma = 7/5$. Fold is along $v^2 = 1$. The upper supersonic branch S_r is repelling while the lower subsonic branch S_a is attracting. For $v < 0$, the manifold is a mirror image of this manifold in the plane $v = 0$ with the same properties.

3.2 Reduced problem

The phase space of the reduced problem (3.4) is the critical manifold S. Since this manifold is given as a graph over (s, v)-space, we project the reduced flow onto this single coordinate chart. We take the total derivative of $f(s, n, v, 0) = 0$ with respect to the slow scale y to obtain the reduced system (3.4) in the (s, v)-chart:

$$\begin{aligned} \frac{ds}{dy} &= g_1(s, n, v, 0) \\ -f_v \frac{dv}{dy} &= f_s g_1(s, n, v, 0) + f_n g_2(s, n, v, 0) \,. \end{aligned} \tag{3.7}$$

Using the definitions of the partial derivatives of f and dividing out a common factor in the second equation we obtain the following reduced problem in the coordinate chart (s, v):

$$\begin{aligned} \frac{ds}{dy} &= \pm 1 \\ \pm\left(\frac{1}{v} - v\right)\frac{dv}{dy} &= \frac{1}{s}\left((1-\gamma)v^2 - 2 + (\gamma+1)\frac{\alpha}{s\bar{c}^2}\right) \,, \end{aligned} \tag{3.8}$$

where

$$\frac{1}{s\bar{c}^2} = \left(\frac{1}{s}\right)^{\frac{5-3\gamma}{\gamma+1}} \left(\frac{1}{|v|}\right)^{-\frac{2(\gamma-1)}{\gamma+1}} \,.$$

Obviously, there are no equilibria in the reduced problem (3.8) reflecting the nonautonomous nature of the original problem. On the other hand, this system is singular along the sonic fold curve $v^2 = 1$. We desingularize the system by the rescaling

$dy = \pm s(\frac{1}{v} - v)d\bar{y}$ which gives the *desingularized system*

$$\begin{aligned} \frac{ds}{d\bar{y}} &= s\left(\frac{1}{v} - v\right) \\ \frac{dv}{d\bar{y}} &= (1-\gamma)v^2 - 2 + (\gamma+1)\frac{\alpha}{s\bar{c}^2}\,. \end{aligned} \tag{3.9}$$

The phase portraits of the reduced and desingularized system are equivalent up to a change of orientation in the supersonic domain, i.e., $v^2 > 1$.

Equilibria of the desingularized system (3.9) are called *folded singularities* and are classified by type according to the eigenvalues of the linearization of (3.9) [22, 2]. If we use the k_r given by (2.8) which is well-defined for $1 \le \gamma < 5/3$ and fixes $\alpha = 1$ then there is a folded singularity at

$$(s^*, v^*) = (1, \pm 1). \tag{3.10}$$

This fact illustrates the advantage of using the length scale k_r (2.8) in the analysis. In contrast, if we use the scale $k_r = r_0$ (2.12) which is well-defined for all $1 \le \gamma \le 5/3$ then the folded singularity occurs at

$$(s^*, v^*) = (\alpha^{\frac{\gamma+1}{5-3\gamma}}, \pm 1)\,. \tag{3.11}$$

Definition 3.1. *The folded singularity* (3.10)*, respectively* (3.11)*, is known as the* sonic point *in the astrophysical literature.*

Remark 3.2. *Recall that the length scale k_r defined in* (2.8) *diverges for subsonic outflow as $\gamma \to 5/3$ from below. Hence the physical location of the sonic point* (3.11) *moves further and further from the star, a result consistent with the fact that a subsonic wind with $\gamma = 5/3$ never becomes supersonic in the absence of energy or momentum injection [16]. The result is confirmed using the length scale* (2.12) *for which the location of the sonic point is given $s^* = \alpha^{\frac{\gamma+1}{5-3\gamma}}$, a quantity that also diverges as $\gamma \to 5/3$ since, as already noted, $\alpha > 1$. Thus the case $\gamma = 5/3$ can be excluded from the transonic flow problem.*

Proposition 3.2. *In the range $1 \le \gamma < 5/3$ of the adiabatic index, the folded singularity* (3.11) *is of saddle type.*

Proof. We calculate the Jacobian of the desingularised system (3.9) evaluated at the folded singularity (3.11):

$$\begin{aligned} J &= \left.\begin{pmatrix} \left(\frac{1}{v} - v\right) & s\left(-\frac{1}{v^2} - 1\right) \\ (\gamma+1)\frac{\partial}{\partial s}\left(\frac{\alpha}{s\bar{c}^2}\right) & 2(1-\gamma)v + (\gamma+1)\frac{\partial}{\partial v}\left(\frac{\alpha}{s\bar{c}^2}\right) \end{pmatrix}\right|_{(s^*,v^*)} \\ &= \begin{pmatrix} 0 & -2\alpha^{\frac{\gamma+1}{5-3\gamma}} \\ (3\gamma-5)\alpha^{\frac{2\gamma-6}{5-3\gamma}} & \pm 2(1-\gamma)(1-\alpha) \end{pmatrix}. \end{aligned} \tag{3.12}$$

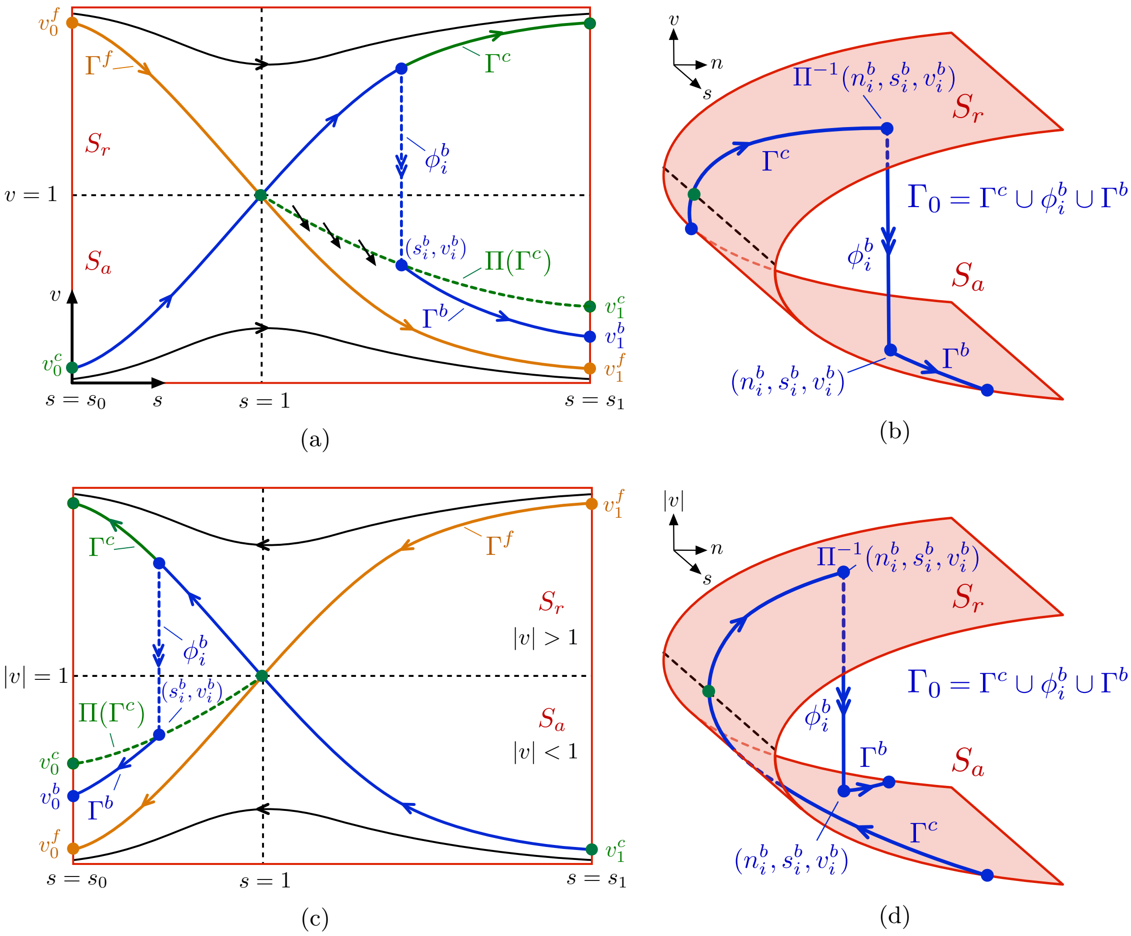

Figure 2: Sketch of the reduced flow projected onto the (s, v)-chart for outflow (top panels) and inflow (bottom panels) including true and faux folded saddle canards and the projection of the upper canard onto S_a. (Note that in the inflow ($v < 0$) diagrams, while the vertical axis represents the absolute value $|v|$, we abuse notation and drop the moduli from the labels of specific v-values.)

The determinant of the Jacobian is given by

$$\det J = \frac{2}{\alpha}(3\gamma - 5) < 0 \quad \text{for } \gamma < \frac{5}{3},$$

and hence the singularity (3.11) is a folded saddle [22]. $\square$

Remark 3.3. *This result again highlights the special role of the limit $\gamma \to 5/3$, this time responsible for the presence of a zero eigenvalue. Note how the Jacobian simplifies for $\alpha = 1$, i.e., when the sonic point is defined by* (3.10)*.*

By looking at the first row of the Jacobian we notice that the eigenvector of the negative eigenvalue of the folded saddle always has a positive slope while the eigenvector of the positive eigenvalue always has negative slope; see Figure 2, upper panels. Note that the symmetry ($v \leftrightarrow -v, \bar{y} \leftrightarrow -\bar{y}$) in (3.9) implies that it suffices to show phase portraits for $v > 0$. We identify two specific solutions that cross the sonic point, a *canard* (from sub- to supersonic), which we denote by Γ^c, and a *faux canard* (super- to subsonic) which we denote by Γ^f, of folded saddle type [2, 22]. The canards are of particular interest since they can be related to stellar wind and stellar accretion with supersonic speed. Eventually, these solutions must become subsonic again, either in the far-field for stellar winds or close to the stellar object for accretion. The only way this can be accomplished is via a jump (shock) from the supersonic to the subsonic branch. For this we have to project the canard from S_r onto S_a; see Figure 2, upper panels. Hence we have to concatenate solutions of the reduced problem (Γ^c, Γ^b) and the layer problem (ϕ_i^b) to construct singular limit solutions $\Gamma_0 = \Gamma^c \cup \phi_i^b \cup \Gamma^b$ that fulfill the prescribed subsonic boundary conditions for our transonic flow problem; see Figure 2.

4 Existence of stellar wind/accretion solutions

In this section, we construct transonic stellar wind/accretion solutions using the above geometric singular perturbation theory framework. As stated in section 2, we construct solutions on a finite interval $s \in [s_0, s_1]$. The general idea of the existence proof is to choose one-dimensional boundary manifolds in the planes $s = s_0$ and $s = s_1$ and follow these forward (resp. backward) under the flow of (3.2), tracing out two-dimensional manifolds. We then show that these manifolds intersect transversely along a one-dimensional trajectory, giving the desired solution, which concludes the proof of Theorem 2.1.

Remark 4.1. *We focus first on the isothermal case $\gamma = 1$ which is easier owing to constant sound speed and then deal with the case $1 < \gamma < 5/3$. In both cases, we use the definition* (2.8) *of k_r that fixes the sonic point at $(s^*, v^*) = (1, \pm 1)$.*

4.1 The case $\gamma = 1$

Our starting point is the desingularized problem (3.9) which in the case of $\gamma = 1$ and $\alpha = 1$ reduces to

$$\begin{aligned} \frac{ds}{d\bar{y}} &= s\left(\frac{1}{v} - v\right) \\ \frac{dv}{d\bar{y}} &= 2\left(\frac{1}{s} - 1\right) \ . \end{aligned} \tag{4.1}$$

System (4.1) is conservative with

$$E(s, v) := 2\left(\ln s + \frac{1}{s}\right) + \ln|v| - \frac{v^2}{2} \tag{4.2}$$

as a conserved quantity, i.e., solutions of (4.1) evolve along level curves $E(s, v) =$ constant. Canards pass through the sonic point $(s^*, v^*) = (1, \pm 1)$, i.e., they correspond to the level curves given by $E(s,v) = \dfrac{3}{2}$. The two saddle canards, the true canard Γ^c and the faux canard Γ^f, partition the (s,v) phase space into four sectors (note that the position of Γ^c, Γ^f depend on whether we are considering the inflow or outflow problem; see Figure 2). Note that E evaluated along the fold line $|v| = 1$ has a minimum at the sonic point, while it has a maximum at the sonic point when evaluated along $s = 1$, another indicator of the saddle structure. Thus, level curves $E(s,v) = \text{constant} > 3/2$ can be found in the (left and right) sectors bounded by the canards that include the fold $|v| = 1$ while the other two (upper and lower) sectors correspond to level curves $E(s,v) = \text{constant} < 3/2$.

We wish to find the projection of the canard segment Γ^c along the repelling branch S_r onto the attracting branch S_a. We define $\Pi : S_r \to S_a$ to be the map which projects from the repelling branch S_r along the one-dimensional fast fibers to the corresponding point on the attracting branch S_a. We note that for $\gamma = 1$, the folded critical manifold is defined by the equation

$$0 = f(s,n,v,0) := -n + \frac{1}{s^2|v|} + \frac{|v|}{s^2} \tag{4.3}$$

which is quadratic in v, and so we can find the $S_{a/r}$ branches of the folded critical manifold as the graphs

$$|v_r(n,s)| = \frac{ns^2 + \sqrt{n^2s^4 - 4}}{2}, \quad |v_a(n,s)| = \frac{ns^2 - \sqrt{n^2s^4 - 4}}{2}. \tag{4.4}$$

Note the symmetry $v \leftrightarrow \dfrac{1}{v}$ in (4.3) which implies that the roots in (4.4) are related by $|v_{a/r}| = |v_{r/a}|^{-1}$. Thus the projection of a point $(n,s,v_r(n,s)) \in S_r$ along a layer solution onto S_a is given by

$$\Pi(n,s,v_r(n,s)) = \big(n,s,v_a(n,s) = v_r^{-1}(n,s)\big) .$$

4.1.1 Stellar wind solutions: $v > 0$

For the stellar wind (outflow) case, the true canard Γ^c is subsonic ($v < 1$) for $s < 1$ and supersonic ($v > 1$) for $s > 1$; see Figure 2a. The goal is to construct a solution which follows Γ^c crossing over the sonic point $(s^*, v^*) = (1,1)$ from S_a to S_r before returning to S_a via a fast jump; see Figure 2b. We will need the following

Lemma 4.1. *The projection of the canard segment Γ^c for $s > 1$ onto S_a lies above the faux canard trajectory Γ^f on S_a, i.e., in the (right) sector with level curves $E(s,v) =$ constant $> 3/2$, and it crosses level curves transversally.*

Proof. The projection of any trajectory defined by $E(s,v) = \text{constant}$ in S_r, i.e., for $v > 1$, is given by replacing v with $1/v$ in $E(s,v)$ defined in (4.2). We compute

$$\frac{d}{d\bar{y}}E(s,v^{-1}) = -2v\left(1 - \frac{1}{s}\right)\left(1 - \frac{1}{v^2}\right)^2 \tag{4.5}$$

which is positive for $s < 1$ and negative for $s > 1$ (independent of $v > 1$) and shows that these projections are not solutions of the reduced problem (4.1), i.e., a projection curve of a level set in S_r onto S_a crosses level curves in S_a transversally.

Note that s as a function of $\bar{y}$ is decreasing for $v > 1$ in (4.1). This implies that we have to reverse the sign in (4.5) to deduce properties of the projection curves from S_r onto S_a in (s, v) phase space. In this phase space, E is strictly increasing along the projection of the canard segment $\Pi(\Gamma^c)$ from S_r onto S_a and for $s > 1$, i.e., $\Pi(\Gamma^c)$ lies in the (right) sector of level curves $E > 3/2$ and hence above the faux canard trajectory Γ^f on S_a, see Figure 2a. □

We denote by v_0^c and v_0^f the v coordinates at which the curves Γ^c and Γ^f approach the boundary $s = s_0$, and denote by v_1^c and v_1^f the v coordinates at which the curves $\Pi(\Gamma^c)$ and Γ^f reach the boundary $s = s_1$, respectively; see Figure 2a. For each $v_1^b \in (v_1^f, v_1^c)$, there exists a trajectory Γ^b of the reduced flow satisfying $v = v_1^b$ at $s = s_1$ which intersects $\Pi(\Gamma^c)$ transversely at some $s = s_i^b > 1$ and $v = v_i^b < 1$. This transverse intersection follows from the fact that E is conserved for the reduced flow and is strictly increasing along $\Pi(\Gamma^c)$. Let n_i^b be the corresponding n coordinate for this intersection in the full system. At this point of intersection, there is a layer solution ϕ_i^b which hits S_r at the point $\Pi^{-1}(n_i^b, s_i^b, v_i^b)$ which lies on Γ^c; see Figure 2b.

Also, for each $v_1^b \in (0, v_1^f)$, there exists a trajectory Γ^b of the reduced flow which reaches $v = v_1^b$ at $s = s_1$ and approaches $v = v_0^b$ at $s = s_0$ for some $v_0^b \in (0, v_0^c)$ and is subsonic for all $s \in (s_0, s_1)$. We have the following proposition regarding the existence of stellar wind solutions; the setup is shown in Figures 2a and 2b.

Proposition 4.1. *Fix $s_0 < 1 < s_1$ and $\gamma = 1$, with v_0^c, v_0^f, v_1^c and v_1^f defined as above, and consider (3.2).*

(i) Let $v_1^b \in (0, v_1^f)$ and let $\Gamma_0 = \Gamma^b$ be the singular subsonic trajectory which approaches $v = v_1^b$ at $s = s_1$. For each sufficiently small $\varepsilon > 0$, Γ_0 perturbs to a solution $\Gamma(\varepsilon)$ of (3.2) which is $\mathcal{O}(\varepsilon)$-close to Γ_0.

(ii) Let $v_1^b \in (v_1^f, v_1^c)$ and let $\Gamma_0 = \Gamma^c \cup \phi_i^b \cup \Gamma^b$ be the singular trajectory which follows Γ^c from $s = s_0$ to $s = s_i^b$, undergoes a fast jump ϕ_i^b at $s = s_i^b$, and then follows the trajectory Γ^b from $s = s_i^b$ to $s = s_1$ (see Figure 2a, 2b). Then for each sufficiently small $\varepsilon > 0$, Γ_0 perturbs to a solution $\Gamma(\varepsilon)$ of (3.2) which is $O(\varepsilon^{1/2})$-close to Γ_0.

Proof. For (i), in the plane $s = s_1$, we define the one-dimensional affine boundary manifold $B_1 := \bar{B}_1 + \gamma_1^b$, where γ_1^b denotes the location of the solution Γ^b at the boundary $s = s_1$, and $\bar{B}_1$ is any line which for $\epsilon = 0$ transversely intersects the manifold S_a at γ_1^b.

We note that Γ_0 is always subsonic for the reduced flow (and hence always on S_a) and bounded away from the fold. Since S_a is normally hyperbolic away from the fold, by Fenichel theory, S_a perturbs to a locally invariant manifold $S_{a,\varepsilon}$ for sufficiently small $\varepsilon > 0$ and the flow on $S_{a,\varepsilon}$ is an $\mathcal{O}(\varepsilon)$ perturbation of the slow flow. Thus the boundary manifold B_1 intersects $S_{a,\epsilon}$ transversely and following this intersection backwards under the flow of (3.2) traces out a solution $\Gamma(\epsilon)$ which is $\mathcal{O}(\epsilon)$-close to Γ_0.

For (ii), by Lemma 4.1, the curves $\Pi(\Gamma^c)$ and Γ^b intersect transversely on S_a for $\varepsilon = 0$. Equivalently, for $\epsilon = 0$, the unstable foliation $\mathcal{W}^u(\Gamma^c)$ of the singular canard trajectory Γ^c on S_r for $s > 1$ transversely intersects the stable foliation $\mathcal{W}^s(\Gamma^b)$ of Γ^b along the fast jump ϕ_i^b. The idea of the proof is to follow two boundary manifolds, B_0 at $s = s_0$ and B_1 at $s = s_1$, forwards (resp. backwards) under the flow of (3.2) for $\epsilon > 0$ and show that these trace out manifolds which are close to $\mathcal{W}^u(\Gamma^c)$ and $\mathcal{W}^s(\Gamma^b)$, respectively, and hence also intersect transversely along the desired solution.

Away from the fold, the manifolds S_a and S_r are normally hyperbolic and hence for sufficiently small $\epsilon > 0$ perturb to locally invariant manifolds $S_{a,\epsilon}$ and $S_{r,\epsilon}$, as do their stable (resp. unstable) foliations. In [22], it was shown that for sufficiently small $\varepsilon > 0$, the singular canard Γ^c perturbs to a trajectory $\Gamma^c(\varepsilon)$ which passes $O(\varepsilon^{1/2})$-close to the sonic point (folded saddle), and in a neighborhood of the fold, the manifolds $S_{a,\varepsilon}$ and $S_{r,\varepsilon}$ intersect transversely along this perturbed canard solution $\Gamma^c(\varepsilon)$.

In the plane $s = s_0$, we define the one-dimensional affine boundary manifold $B_0 := \bar{B}_0 + \gamma^c(\epsilon)$, where $\gamma^c(\epsilon)$ denotes location of the maximal canard $\Gamma^c(\varepsilon)$ at the boundary $s = s_0$, and $\bar{B}_0$ is any line transverse to the $\epsilon = 0$ fast stable fiber $\mathcal{W}^s(\gamma^c(0))$ of $\gamma^c(0)$ at $s = s_0$.

Following the boundary manifold B_0 forward along $\Gamma_c(\varepsilon)$ traces out a two-dimensional manifold B_0^* which is exponentially close to $S_{a,\varepsilon}$ upon entering a neighborhood of the fold. Since the manifolds $S_{a,\varepsilon}$ and $S_{r,\varepsilon}$ intersect transversely along the perturbed canard solution $\Gamma^c(\varepsilon)$ and B_0^* is exponentially close to $S_{a,\varepsilon}$ upon entering this neighborhood, we have that B_0^* also intersects $S_{r,\varepsilon}$ transversely along $\Gamma^c(\varepsilon)$. Since this intersection is transverse, the exchange lemma [14] implies that upon entry into a neighborhood of $s = s_i^b$, B_0^* aligns exponentially close with the strong unstable fibers $\mathcal{W}^u(\Gamma^c(\varepsilon))$ of the canard trajectory $\Gamma^c(\varepsilon)$; hence B_0^* is $\mathcal{O}(\epsilon)$-close to $\mathcal{W}^u(\Gamma^c)$.

We define the one-dimensional boundary manifold B_1 at $s = s_1$ as above in the proof of part (i). Since B_1 intersects S_a transversely for $\epsilon = 0$, this persists for $\epsilon > 0$ as a transverse intersection between B_1 and $S_{a,\varepsilon}$. Following B_1 backwards traces out a two-dimensional manifold B_1^*, which, by the exchange lemma, aligns exponentially close to the unstable fibers of a slow trajectory on $S_{a,\epsilon}$ which is $\mathcal{O}(\epsilon)$ close to Γ_b. Thus B_1^* is $\mathcal{O}(\epsilon)$-close to $\mathcal{W}^s(\Gamma^b)$ in a neighborhood of $s = s_i^b$.

By the transversality of the intersection of $\mathcal{W}^u(\Gamma^c)$ and $\mathcal{W}^s(\Gamma^b)$ along ϕ_i^b for $\varepsilon = 0$, for sufficiently small $\varepsilon > 0$, there is a transverse intersection of the two-dimensional manifolds B_0^* and B_1^* along the desired trajctory $\Gamma(\epsilon)$.

□

4.1.2 Stellar accretion solutions: $v < 0$

In this section, we consider the inflow problem for $v < 0$; the setup is shown in Figures 2c and 2d. Much of the analysis from the previous section carries over, although the flow on the critical manifold is reversed and hence the true canard and faux canard switch places. We abuse notation and denote by Γ^c the corresponding canard solution and by Γ^f the faux canard (despite the switch in their location, see Figure 2). For the inflow case, the true canard Γ^c is subsonic ($|v| < 1$) for $s > 1$ and supersonic ($|v| > 1$) for $s < 1$.

We now consider solutions which start in the far field ($s > 1$) and follow Γ^c crossing over the sonic point $(s^*, v^*) = (1, -1)$ from S_a to S_r before returning to S_a via a fast jump (see Figure 2d). The following lemma is proved similarly to Lemma 4.1.

Lemma 4.2. *The projection of the canard segment Γ^c for $0 < s < 1$ onto S_a lies above the canard trajectory Γ^f on S_a, i.e., in the (left) sector with level curves $E(s, v) =$ constant $> 3/2$, and it crosses level curves transversally.*

We denote by v_0^c and v_0^f the v coordinates at which the curves $\Pi(\Gamma^c)$ and Γ^f approach the boundary $s = s_0$, and denote by v_1^c and v_1^f the v coordinates at which the curves Γ^c and Γ^f reach the boundary $s = s_1$, respectively. For each $v_0^b \in (v_0^c, v_0^f)$, there exists a trajectory Γ^b of the reduced flow satisfying $v = v_0^b$ at $s = s_0$ which intersects $\Pi(\Gamma^c)$ transversely at some $s = s_i^b < 1$ and $v = v_i^b > -1$. Let n_i^b be the corresponding n coordinate for this intersection in the full system. At this point of intersection, there is a layer solution ϕ_i^b which hits S_r at the point $\Pi^{-1}(n_i^b, s_i^b, v_i^b)$ which lies on Γ^c.

Also, for each $v_0^b \in (v_0^f, 0)$, there exists a trajectory Γ^b of the reduced flow which reaches $v = v_0^b$ at $s = s_0$ and approaches $v = v_1^b$ at $s = s_1$ for some $v_1^b \in (v_1^c, 0)$ and is subsonic for all $s \in (s_0, s_1)$. We have the following proposition regarding the existence of stellar accretion solutions.

Proposition 4.2. *Fix $s_0 < 1 < s_1$ and $\gamma = 1$, with v_0^c, v_0^f, v_1^c and v_1^f defined as above, and consider (3.2).*

(i) Let $v_0^b \in (v_0^f, 0)$ and let $\Gamma_0 = \Gamma^b$ be the singular subsonic trajectory which approaches $v = v_0^b$ at $s = s_0$. For each sufficiently small $\varepsilon > 0$, Γ_0 perturbs to a solution $\Gamma(\varepsilon)$ of (3.2) which is $\mathcal{O}(\varepsilon)$-close to Γ_0.

(ii) Let $v_0^b \in (v_0^c, v_0^f)$ and let $\Gamma_0 = \Gamma^c \cup \phi_i^b \cup \Gamma^b$ be the singular trajectory which follows Γ^c from $s = s_1$ to $s = s_i^b$, undergoes a fast jump ϕ_i^b at $s = s_i^b$, and then follows the trajectory Γ^b from $s = s_i^b$ to $s = s_0$ (see Figures 2c, 2d). Then for each sufficiently small $\varepsilon > 0$, Γ_0 perturbs to a solution $\Gamma(\varepsilon)$ of (3.2) which is $O(\varepsilon^{1/2})$-close to Γ_0.

Proof. The proof is similar to that of Proposition 4.1. □

4.2 The general case $1 < \gamma < 5/3$

We first note that for $1 < \gamma < 5/3$, the dimensionless energy

$$\bar{E} := \frac{1}{2}\bar{c}^2 v^2 + \frac{\bar{c}^2}{\gamma - 1} - \frac{2}{s} \tag{4.6}$$

is conserved in the desingularized system (3.9). Thus along a canard solution passing through the sonic point $(s^*, v^*) = (1, \pm 1)$, we have that

$$\frac{1}{2}\bar{c}^2 v^2 + \frac{\bar{c}^2}{\gamma - 1} - \frac{2}{s} = \frac{1}{\gamma - 1} - \frac{3}{2} \tag{4.7}$$

which, after some rearranging, reduces to

$$\left(\frac{v^2}{2}+\frac{1}{\gamma-1}\right)\left(\frac{1}{v^2}\right)^{\frac{\gamma-1}{\gamma+1}}=\left(\frac{1}{\gamma-1}-\frac{3}{2}+\frac{2}{s}\right)s^{\frac{4(\gamma-1)}{\gamma+1}}\ . \tag{4.8}$$

We implicitly differentiate with respect to s to obtain

$$\frac{dv}{ds}=\frac{(5-3\gamma)s^{\frac{2(\gamma-3)}{\gamma+1}}(s-1)}{v^{\frac{1-3\gamma}{\gamma+1}}(v^2-1)}\ . \tag{4.9}$$

Using L'Hôpital's rule, we see that the flow bifurcates in two directions at the sonic point $(s^*,v^*)=(1,\pm1)$, along the canard and faux-canard curves with

$$\left.\frac{dv}{ds}\right|_{(s,v)=(1,\pm1)}=\pm\sqrt{\frac{5-3\gamma}{2}}\ . \tag{4.10}$$

The folded critical manifold is defined by

$$0=f(s,n,v,0):=\left(\frac{\gamma+1}{2}\right)\frac{1}{\bar{c}}\left(-n+\bar{\rho}\bar{c}^2v^2+\bar{p}\right)\ , \tag{4.11}$$

or equivalently

$$\left(\frac{1}{v^2}\right)^{\frac{\gamma}{\gamma+1}}\left(\gamma v^2+1\right)=\gamma n s^{\frac{4\gamma}{\gamma+1}}\ . \tag{4.12}$$

We again define $\Pi : S_r \to S_a$ to be the map which projects from the repelling branch S_r along the one-dimensional fast fibers to the corresponding point on the attracting branch S_a. For a point $(n,s,v(n,s))$ on S_r, i.e., $|v|>1$, there is a fast layer solution between S_r and S_a. We compute that the corresponding coordinate projected along this layer solution onto S_a is given by $\Pi(n,s,v(n,s))=(n,s,\tilde{v}(n,s))$, where $|\tilde{v}(n,s)|<1$ can be defined implicitly by the equation

$$\left(\frac{1}{\tilde{v}^2}\right)^{\frac{\gamma}{\gamma+1}}\left(\gamma\tilde{v}^2+1\right)=\left(\frac{1}{v^2}\right)^{\frac{\gamma}{\gamma+1}}\left(\gamma v^2+1\right)\ , \tag{4.13}$$

where we used (4.12).

4.2.1 Stellar wind solutions: $v>0$

Proceeding as in 4.1, for the stellar wind (outflow) case, we define Γ^c to be the outgoing canard trajectory [subsonic ($v<1$) for $s<1$ and supersonic ($v>1$) for $s>1$] and Γ^f to be the corresponding faux canard trajectory. The goal is to construct a solution which follows Γ^c crossing over the sonic point $(s^*,v^*)=(1,1)$ from S_a to S_r before returning to S_a via a fast jump (see Figure 2b). We are concerned with the nature of the projection $\Pi(\Gamma^c)$ which is summed up in the following

Lemma 4.3. *Let $1 < \gamma < 5/3$, and consider the projection $\Pi(\Gamma^c)$ of the outgoing canard trajectory Γ^c from S_r to S_a. For $s > 1$, the following hold*

(i) The projected curve $\Pi(\Gamma^c)$ lies strictly above the faux canard Γ^f.

(ii) The curve $\Pi(\Gamma^c)$ is transverse to the reduced flow on the branch S_a.

Proof. For (i), we note that the canard Γ^c and Γ^f lie on the same $\bar{E}$-level. For a point (s, v) on Γ^c, we denote by $\hat{v} < 1$ the v-coordinate so that $(s, \hat{v})$ lies on Γ^f, that is, (s, v) and $(s, \hat{v})$ are on the same $\bar{E}$-level. We recall that the v-coordinate of the projected curve $\Pi(\Gamma^c)$ is denoted by $\tilde{v}$; thus we aim to show that $\tilde{v} > \hat{v}$ for $s > 1$. Using (4.13), we implicitly differentiate with respect to v and compute

$$\frac{d\tilde{v}}{dv} = D(v, \tilde{v}) := \frac{v^{-\frac{3\gamma+1}{\gamma+1}}\left(v^2 - 1\right)}{\tilde{v}^{-\frac{3\gamma+1}{\gamma+1}}\left(\tilde{v}^2 - 1\right)} < 0 \ . \tag{4.14}$$

Using the fact that Γ^c and Γ^f lie on the same $\bar{E}$ level, we can use the energy equation (4.8) to define $\hat{v}$ implicitly as

$$\left(\frac{\hat{v}^2}{2} + \frac{1}{\gamma - 1}\right)\left(\frac{1}{\hat{v}^2}\right)^{\frac{\gamma-1}{\gamma+1}} = \left(\frac{v^2}{2} + \frac{1}{\gamma - 1}\right)\left(\frac{1}{v^2}\right)^{\frac{\gamma-1}{\gamma+1}} \quad , \tag{4.15}$$

which we differentiate to obtain

$$\frac{d\hat{v}}{dv} = \frac{v^{\frac{1-3\gamma}{\gamma+1}}}{\hat{v}^{\frac{1-3\gamma}{\gamma+1}}}\left(\frac{v^2 - 1}{\hat{v}^2 - 1}\right) < D(v, \hat{v}) \ . \tag{4.16}$$

Thus we have that

$$\frac{d\tilde{v}}{dv} - \frac{d\hat{v}}{dv} > D(v, \tilde{v}) - D(v, \hat{v}) = \partial_2 D(v, \zeta(v))(\tilde{v} - \hat{v}) \,, \tag{4.17}$$

for some function $\zeta(v)$. We can also write

$$\frac{d\tilde{v}}{dv} - \frac{d\hat{v}}{dv} = \partial_2 D(v, \zeta(v))(\tilde{v} - \hat{v}) + \omega(v) \tag{4.18}$$

for some function ω satisfying $\omega(v) > 0$ for $v > 1$. Define

$$\kappa(v) = \int_1^v \partial_2 D(u, \zeta(u)) du \ , \tag{4.19}$$

and note that at $v = 1$, we have $\tilde{v} = \hat{v} = 1$. We therefore have that

$$\tilde{v}(v) - \hat{v}(v) = \int_1^v e^{\kappa(v) - \kappa(u)}\omega(u) du > 0 \ , \tag{4.20}$$

as claimed.

For (ii), we proceed by showing transversality of the projection Γ^c with respect to the constant $\bar{E}$ curves which define the reduced flow on S_r. For $s > 1$, we consider the projection $\Pi(\Gamma^c)$ as a graph $\tilde{v}(s)$. Using equations (3.9) with $\alpha = 1$, we compute the slope of the reduced flow at a point (s, v) as

$$\frac{dv}{ds} = \frac{(\gamma-1)v^{\frac{2}{\gamma+1}} + 2v^{-\frac{2\gamma}{\gamma+1}} - (\gamma+1)s^{\frac{3\gamma-5}{\gamma+1}} v^{-\frac{2}{\gamma+1}}}{s v^{-\frac{3\gamma+1}{\gamma+1}} (v^2 - 1)} \ . \tag{4.21}$$

To compute the slope of $\Pi(\Gamma^c)$, we write

$$\frac{d\tilde{v}}{ds} = \frac{d\tilde{v}}{dv}\frac{dv}{ds} = \frac{(\gamma-1)v^{\frac{2}{\gamma+1}} + 2v^{-\frac{2\gamma}{\gamma+1}} - (\gamma+1)s^{\frac{3\gamma-5}{\gamma+1}} v^{-\frac{2}{\gamma+1}}}{s \tilde{v}^{-\frac{3\gamma+1}{\gamma+1}} (\tilde{v}^2 - 1)} \ . \tag{4.22}$$

At a point $(s, \tilde{v})$, we now compare the slope of $\Pi(\Gamma^c)$ with that of the reduced flow as

$$\begin{aligned} \frac{d\tilde{v}}{ds} - \left.\frac{dv}{ds}\right|_{(s,v)=(s,\tilde{v})} &= \frac{(\gamma-1)\left(\tilde{v}^{\frac{2}{\gamma+1}} - v^{\frac{2}{\gamma+1}}\right) + 2\left(\tilde{v}^{-\frac{2\gamma}{\gamma+1}} - v^{-\frac{2\gamma}{\gamma+1}}\right)}{s\tilde{v}^{-\frac{3\gamma+1}{\gamma+1}}(1-\tilde{v}^2)} + \\ &\quad \frac{(\gamma+1)s^{\frac{3\gamma-5}{\gamma+1}}\left(v^{-\frac{2}{\gamma+1}} - \tilde{v}^{-\frac{2}{\gamma+1}}\right)}{s\tilde{v}^{-\frac{3\gamma+1}{\gamma+1}}(1-\tilde{v}^2)} \\ &= \frac{(\gamma+1)\left(v^{\frac{2}{\gamma+1}} - \tilde{v}^{\frac{2}{\gamma+1}}\right)\left((v\tilde{v})^{\frac{2}{\gamma+1}} - s^{\frac{3\gamma-5}{\gamma+1}}\right)}{s\,(v\tilde{v})^{\frac{2}{\gamma+1}}\,\tilde{v}^{-\frac{3\gamma+1}{\gamma+1}}(1-\tilde{v}^2)} \ , \end{aligned}$$

where we used (4.13). We claim that the difference in slope is positive for $v > 1$. For $v > 1$, we have $\tilde{v} < 1$; hence, provided that

$$v\tilde{v} > s^{\frac{3\gamma-5}{2}} \tag{4.23}$$

is satisfied for all $v > 1$, we obtain the desired transversality. We note that at $v = s = 1$, we have that $v\tilde{v} = s^{\frac{3\gamma-5}{2}} = 1$ and

$$\begin{aligned} \frac{d}{ds}\left(s^{\frac{3\gamma-5}{2}}\right)\bigg|_{s=1} &= \frac{3\gamma-5}{2} < 0 \\ \frac{d}{ds}(v\tilde{v})\bigg|_{(s,v)=(1,1)} &= \frac{d}{dv}(v\tilde{v})\bigg|_{v=1}\ \frac{dv}{ds}\bigg|_{s=1} \ . \end{aligned} \tag{4.24}$$

Using (4.14) and L'Hôpital's rule, we compute that

$$\lim_{v\to1}\frac{d\tilde{v}}{dv} = -1 \ , \tag{4.25}$$

and therefore

$$\frac{d}{dv}(v\tilde{v})\bigg|_{v=1} = \left(\tilde{v} + v\frac{d\tilde{v}}{dv}\right)\bigg|_{v=1} = 0 \ . \tag{4.26}$$

Thus

$$\left.\frac{d}{ds}\left(v\tilde{v}-s^{\frac{3\gamma-5}{2}}\right)\right|_{(s,v)=(1,1)} \quad > \quad 0\ . \tag{4.27}$$

For $v>1$, we have

$$\begin{aligned}\frac{d}{dv}\left(v\tilde{v}\right) &= \frac{d\tilde{v}}{dv}v+\tilde{v} \\ &= \frac{(\gamma-1)\,v^{\frac{4}{\gamma+1}}+2v^{-\frac{2(\gamma-1)}{\gamma+1}}-(1+\gamma)\left(v\tilde{v}\right)^{\frac{2}{\gamma+1}}}{\tilde{v}^{\frac{1-3\gamma}{\gamma+1}}\left(1-\tilde{v}^2\right)}\ .\end{aligned} \tag{4.28}$$

If there exist $s,v>1$ such that $v\tilde{v}=s^{\frac{3\gamma-5}{2}}$, then we have

$$\begin{aligned}\frac{d}{dv}\left(v\tilde{v}\right) &= \frac{\left(5-3\gamma+\frac{4(\gamma-1)}{s}\right)s^{\frac{4(\gamma-1)}{\gamma+1}}-(1+\gamma)s^{\frac{3\gamma-5}{\gamma+1}}}{\tilde{v}^{\frac{1-3\gamma}{\gamma+1}}\left(1-\tilde{v}^2\right)} \\ &= \frac{(5-3\gamma)s^{\frac{3\gamma-5}{\gamma+1}}\left(s-1\right)}{\tilde{v}^{\frac{1-3\gamma}{\gamma+1}}\left(1-\tilde{v}^2\right)} \\ &> 0\ ,\end{aligned} \tag{4.29}$$

where we used (4.8). Since $\dfrac{dv}{ds}>0$ for $s,v>1$, we have

$$\frac{d}{ds}\left(v\tilde{v}-s^{\frac{3\gamma-5}{2}}\right) \quad > \quad 0 \tag{4.30}$$

whenever $v\tilde{v}=s^{\frac{3\gamma-5}{2}}$. Combined with (4.27), we see that we must in fact have $v\tilde{v}>s^{\frac{3\gamma-5}{2}}$ for all $s>1$, which completes the proof of (ii).

□

We now proceed as in Section 4.1 and fix $0<s_0<1<s_1$. We denote by v_0^c and v_0^f the v coordinates at which the curves Γ^c and Γ^f approach the boundary $s=s_0$, and denote by v_1^c and v_1^f the v coordinates at which the curves $\Pi(\Gamma^c)$ and Γ^f reach the boundary $s=s_1$, respectively. The existence of these points follows from the monotonicity of the derivative (4.9) along the canard curves for $s,v\neq 1$. For each $v_1^b\in(v_1^f,v_1^c)$, there exists a trajectory Γ^b of the reduced flow satisfying $v=v_1^b$ at $s=s_1$ which intersects $\Pi(\Gamma^c)$ transversely at some $s=s_i^b>1$ and $v=v_i^b<1$. This transverse intersection follows from Lemma 4.3. Let n_i^b be the corresponding n coordinate for this intersection in the full system. At this point of intersection, there is a layer solution ϕ_i^b which hits S_r at the point $\Pi^{-1}(n_i^b,s_i^b,v_i^b)$ which lies on Γ^c.

Also, for each $v_1^b\in(0,v_1^f)$, there exists a trajectory Γ^b of the reduced flow which reaches $v=v_1^b$ at $s=s_1$ and approaches $v=v_0^b$ at $s=s_0$ for some $v_0^b\in(0,v_0^c)$ and is subsonic for all $s\in(s_0,s_1)$. We have the following

Proposition 4.3. *Fix $s_0 < 1 < s_1$ and $1 < \gamma < 5/3$ with v_0^c, v_0^f, v_1^c, and v_1^f defined as above and consider (3.2).*

(i) Let $v_1^b \in (0, v_1^f)$ and let $\Gamma_0 = \Gamma^b$ be the singular subsonic trajectory which approaches $v = v_1^b$ at $s = s_1$. For each sufficiently small $\varepsilon > 0$, Γ_0 perturbs to a solution $\Gamma(\varepsilon)$ of (3.2) which is $\mathcal{O}(\varepsilon)$-close to Γ_0.

(ii) Let $v_{b,1} \in (v_1^f, v_1^c)$ and let $\Gamma_0 = \Gamma^c \cup \phi_i^b \cup \Gamma^b$ be the singular trajectory which follows Γ^c from $s = s_0$ to $s = s_i^b$, undergoes a fast jump ϕ_i^b at $s = s_i^b$, and then follows the trajectory Γ^b from $s = s_i^b$ to $s = s_1$ (see Figure 2a, 2b). Then for each sufficiently small $\varepsilon > 0$, Γ_0 perturbs to a solution $\Gamma(\varepsilon)$ of (3.2) which is $O(\varepsilon^{1/2})$-close to Γ_0.

Proof. Using the results of Lemma 4.3, statements (i) and (ii) follow from the same arguments as in the proof of Proposition 4.1. □

4.2.2 Stellar accretion solutions: $v < 0$

In this section, we consider the stellar accretion (inflow) problem for $v < 0$. We denote by Γ^c the canard solution and by Γ^f the faux canard. For the inflow case, Γ^c is subsonic ($|v| < 1$) for $s > 1$ and supersonic ($|v| > 1$) for $s < 1$. We consider solutions which start in the far field ($s > 1$) and follow Γ^c crossing over the sonic point $(s^*, v^*) = (1, -1)$ from S_a to S_r before returning to S_a via a fast jump (see Figure 2d). The following lemma is proved similarly to Lemma 4.3

Lemma 4.4. *Let $1 < \gamma < 5/3$, and consider the projection $\Pi(\Gamma^c)$ of the outgoing canard trajectory Γ^c from S_r to S_a. For $s < 1$, the following hold*

(i) The projected curve $\Pi(\Gamma^c)$ lies strictly above the faux canard Γ^f.

(ii) The curve $\Pi(\Gamma^c)$ is transverse to the reduced flow on the branch S_a.

We now proceed as above and denote by v_0^c and v_0^f the v coordinates at which the curves $\Pi(\Gamma^c)$ and Γ^f approach the boundary $s = s_0$, and denote by v_1^c and v_1^f the v coordinates at which the curves Γ^c and Γ^f reach the boundary $s = s_1$, respectively. For each $v_0^b \in (v_0^c, v_0^f)$, there exists a trajectory Γ^b of the reduced flow satisfying $v = v_0^b$ at $s = s_0$ which intersects $\Pi(\Gamma^c)$ transversely at some $s = s_i^b < 1$ and $v = v_i^b > -1$. Let n_i^b be the corresponding n coordinate for this intersection in the full system. At this point of intersection, there is a layer solution ϕ_i^b which hits S_r at the point $\Pi^{-1}(n_i^b, s_i^b, v_i^b)$ which lies on Γ^c.

Also, for each $v_0^b \in (v_0^f, 0)$, there exists a trajectory Γ^b of the reduced flow which reaches $v = v_0^b$ at $s = s_0$ and approaches $v = v_1^b$ at $s = s_1$ for some $v_1^b \in (v_1^c, 0)$ and is subsonic for all $s \in (s_0, s_1)$. We have the following

Proposition 4.4. *Fix $s_0 < 1 < s_1$ and $1 < \gamma < 5/3$ with v_0^c, v_0^f, v_1^c, and v_1^f defined as above and consider (3.2).*

(i) Let $v_1^b \in (v_0^f, 0)$ and let $\Gamma_0 = \Gamma^b$ be the singular subsonic trajectory which approaches $v = v_0^b$ at $s = s_0$. For each sufficiently small $\varepsilon > 0$, Γ_0 perturbs to a solution $\Gamma(\varepsilon)$ of (3.2) which is $\mathcal{O}(\varepsilon)$-close to Γ_0.

(ii) Let $v_{b,0} \in (v_0^c, v_0^f)$ and let $\Gamma_0 = \Gamma^c \cup \phi_i^b \cup \Gamma^b$ be the singular trajectory which follows Γ^c from $s = s_1$ to $s = s_i^b$, undergoes a fast jump ϕ_i^b at $s = s_i^b$, and then follows the trajectory Γ^b from $s = s_i^b$ to $s = s_0$ (see Figure 2c, 2d). Then for each sufficiently small $\varepsilon > 0$, Γ_0 perturbs to a solution $\Gamma(\varepsilon)$ of (3.2) which is $O(\varepsilon^{1/2})$-close to Γ_0.

Proof. Using the results of Lemma 4.4, statements (i) and (ii) follow from the same arguments as in the proof of Proposition 4.1. □

4.3 Proof of Theorem 2.1 (Theorem 1.1)

We conclude the proof of Theorem 2.1 using the analysis of sections 4.1 and 4.2.

Proof of Theorem 2.1. For the outflow problem (i), for each fixed $\gamma \in [1, 5/3)$ and $s_0 < 1 < s_1$, we deduce for sufficiently small $\epsilon > 0$ the existence of transonic stellar wind solutions from Proposition 4.1(ii) for the case of $\gamma = 1$ and from Proposition 4.3(ii) for $1 < \gamma < 5/3$. The existence of the subsonic stellar breeze solutions follows from Propositions 4.1(i) and 4.3(i).

Similarly, for the inflow problem, the assertions in (ii) regarding stellar accretion solutions follow from Propositions 4.2 and 4.4.

The nonexistence of transonic solutions for $\gamma = 5/3$ follows from the fact that the sonic point diverges in this limit; hence no solution can attain supersonic speeds in this case (see Remark 3.2). □

5 PDE numerics

In this section, we compute numerical transonic solutions to Eqs. (1.4) for the outflow (stellar wind) problem. In the dimensionless variables, system (1.4) becomes

$$\begin{aligned} \bar{\rho}_{\bar{t}} + \frac{1}{s^2}\frac{\partial}{\partial s}(\bar{\rho} s^2 \bar{c} v) &= 0, \\ (\bar{\rho}\bar{c}v)_{\bar{t}} + \frac{1}{s^2}\frac{\partial}{\partial s}(\bar{\rho} s^2 \bar{c}^2 v^2) + \frac{\partial \bar{p}}{\partial s} + \frac{2\alpha\bar{\rho}}{s^2} &= \epsilon \frac{\partial}{\partial s}\left(\frac{1}{s^2}\frac{\partial}{\partial s}(s^2 \bar{c} v)\right), \end{aligned} \tag{5.1}$$

where time has been rescaled by $t = \dfrac{k_r}{k_c}\bar{t}$ and we set $\bar{p} = \rho^\gamma/\gamma$.

For the boundary conditions we fix the mass flux at the stellar surface $s = s_0 = 0.33$, i.e., at one third of the critical radius. The equations are solved on a finite domain of length five times the critical radius, i.e., we consider $s \in [0.33, 5.33]$. In the far field, we assume that the flow relaxes to a constant pressure $\bar{p} \to \bar{p}_1$, using a nonreflecting outflow boundary condition [21, 12] at $s = s_1 = 5.33$.

We solve Eqs. (5.1) in MATLAB using a numerical scheme which employs the finite volume method with spherical symmetry for the spatial discretization and MATLAB's

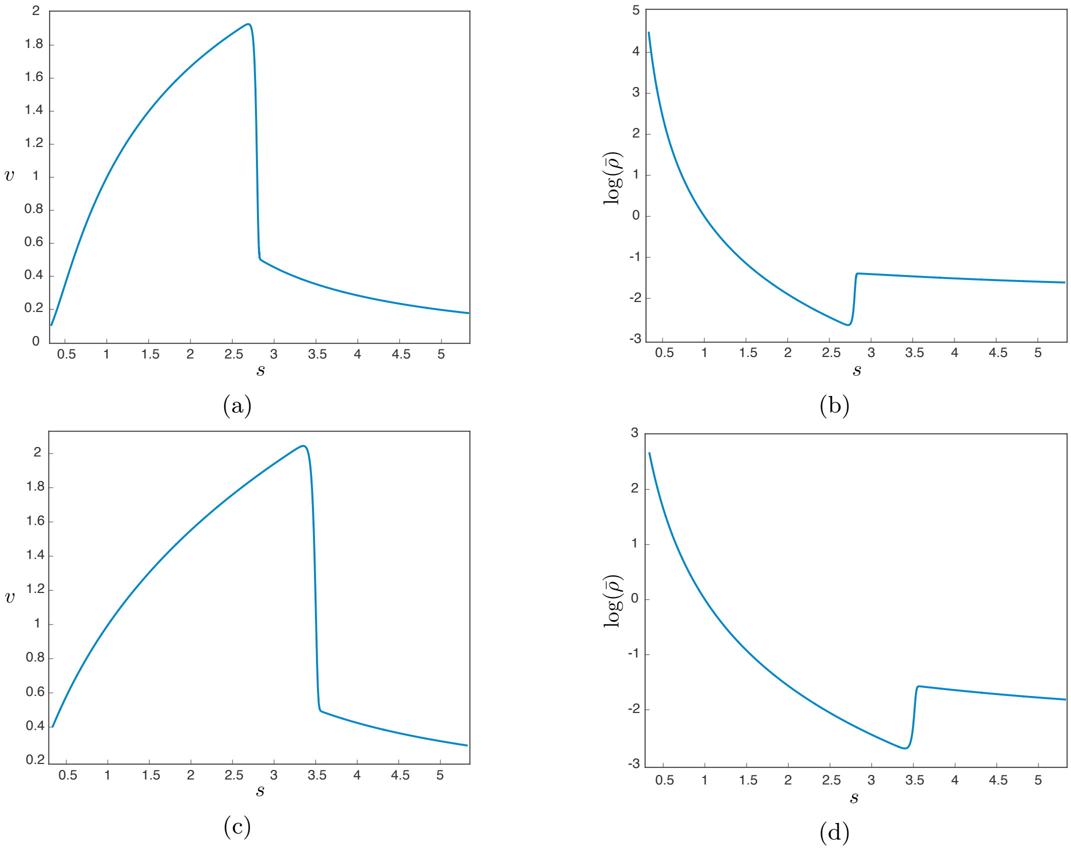

Figure 3: Shown are velocity profiles and log plots of density for transonic stellar wind solutions to (5.1) obtained numerically for the parameter values $\alpha = 1$, $\epsilon = 0.002$, $\gamma = 1$ (top panels) and $\gamma = 4/3$ (bottom panels).

ode45 routine for time integration. Solutions were obtained by time-stepping initial profiles resembling the singular shocks constructed in §4 with the corresponding boundary conditions until a steady state was achieved. The emergence of steady transonic profiles suggests the stability of such solutions in the underlying PDE.

5.1 Transonic stellar wind solutions for $\epsilon > 0$

Figure 3 shows velocity and density profiles obtained for $\alpha = 1$, $\epsilon = 0.002$ for two different values of $\gamma = \{1, 4/3\}$. For $\gamma = 1$, we note that $\bar{c} = 1$, and the boundary conditions are set at $(\bar{\rho}v)_0 = \bar{\rho}v|_{s=0.33} = 9.1$ and the far-field pressure $\bar{p}_1 = 0.2$. For $\gamma = 4/3$ we take $(\bar{\rho}\bar{c}v)_0 = 9.1$ and $\bar{p}_1 = 0.32$.

We now fix $\gamma = \alpha = 1$ and consider the effect of varying the perturbation parameter ϵ. We fix the mass flux $(\bar{\rho}v)_0 = \bar{\rho}v|_{s=0.33} = 9.1$ at the inner boundary, and we take the far-field pressure $\bar{p}_1 = 0.2$. Figure 4 shows stationary velocity and density profiles obtained for these parameters for values of $\epsilon = \{0.002, 0.005, 0.01\}$. These profiles are plotted

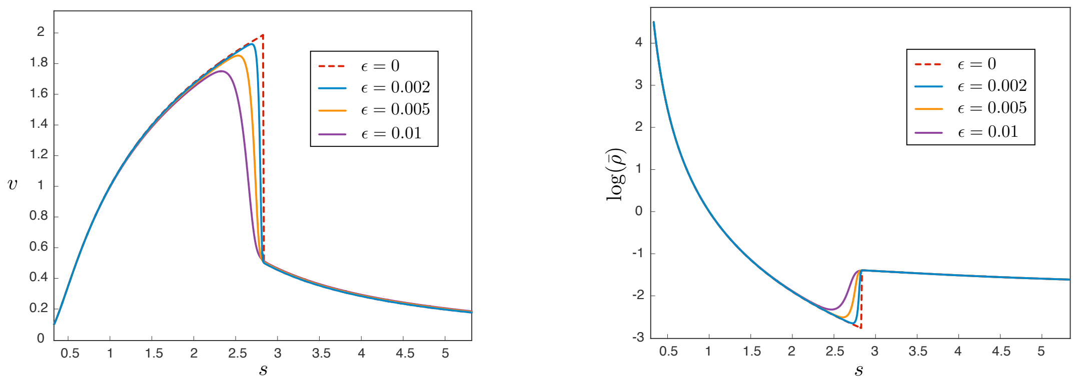

Figure 4: Shown are velocity profiles and log plots of density for transonic stellar wind solutions to (5.1) obtained numerically for the parameter values $\gamma = 1$, $\alpha = 1$, $\epsilon = \{0.002, 0.005, 0.01\}$. Also plotted (dashed red) are the corresponding singular $\epsilon = 0$ profiles (see section 4).

alongside the corresponding singular shock profiles constructed in section 4 satisfying the same boundary conditions. The location of the shock is fixed by the boundary conditions, but as expected the shock becomes gradually steeper and approaches the singular limit as ϵ decreases.

5.2 Dependence on far-field boundary conditions

We now fix $\alpha = \gamma = 1$, $\epsilon = 0.002$ and investigate the effect of varying the far-field pressure boundary condition $\bar{p} \to \bar{p}_1$. The results for values of $\bar{p}_1 = \{0.16, 0.2, 0.27, 0.33, 0.37\}$ are shown in Figure 5. Note that the location of the shock does depend on the far-field pressure and for sufficiently large values of $\bar{p}_1$ there is no shock since the flow does not cross the sonic point. Instead, such conditions result in solutions which are subsonic on the entire interval, i.e., a stellar breeze.

6 Conclusion

In this paper we revisited the classical formulation of the stellar wind problem and the closely related problem of spherical accretion. We have used geometric singular perturbation theory to reinterpret the sonic point as a folded saddle and to identify the associated critical trajectory with the transonic solution first found by E. N. Parker. Our results prove the existence of this trajectory and moreover identify the shock that is expected to terminate the supersonic wind with a canard trajectory whereby the solution departs abruptly from a repelling invariant manifold corresponding to the supersonic part of the solution to an attracting subsonic part. In our description the presence of this layer solution is the result of small but nonzero viscous effects in the flow which allow the solution to connect to the interplanetary medium beyond the termination shock –

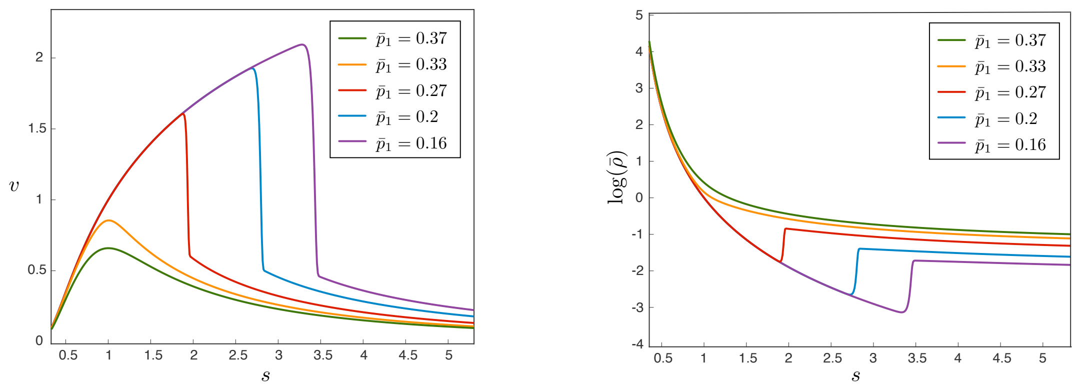

Figure 5: Shown are velocity profiles and log plots of density for transonic stellar wind solutions to (5.1) obtained numerically for the parameter values $\gamma = 1$, $\alpha = 1$, $\epsilon = 0.002$ with far field pressure $\bar{p}_1 = \{0.16, 0.2, 0.27, 0.33, 0.37\}$.

recall that the Voyager 1 spacecraft passed through the termination shock in 2003 [15] – but the details of the solution and in particular the location of the shock are insensitive to the magnitude of the viscosity.

Our formulation of the problem is necessarily idealized. In addition to the assumption of spherical outflow, we have ignored the temperature dependence of dynamic viscosity η. Moreover, we have assumed that the adiabatic gas law (1.2), viz., $p = \beta\rho^\gamma$ holds throughout the flow. It is known, however, that there is always an increase in entropy across a shock, although for weak to moderate shocks this increase is much smaller than the jump in pressure, flow speed or density ([25], Ch. 6). Thus the quantity β must also increase across the shock. Moreover, if the shock is strong and leads to the reionization of the gas then γ will drop. Thus the use of the adiabatic relation $p = \beta\rho^\gamma$ is at best an approximation, albeit one that is frequently employed [8, 16]. In this connection we note that one expects thermal diffusivity to exceed viscosity, an effect we have neglected. With thermal diffusion included one has to give up the adiabatic relation and replace it with the full energy equation, leading to a third order system in place of the second order system studied here (see e.g. [1, 10]). These complications raise interesting mathematical questions in their own right but are beyond the scope of this paper.

Despite the idealized nature of the problem our results shed new light on the mathematical structure of these types of flow. In particular, we have identified folded saddle type canards as the only structure able to describe a sub- to supersonic transition. Such structures have previously been identified in related flows such as transonic flows through a nozzle [9, 18]. Canards have also been associated with shock-fronted travelling wave profiles in advection-reaction-diffusion problems [24] and, in particular, in models of wound healing angiogenesis and solid tumour invasion [6, 7].

It remains to consider the reasons why the flow should select the critical (canard) trajectory. Heuristic arguments [16] suggest that this solution is stable, a prediction that is confirmed in the numerical computation of the outflow profiles in section 5 using a time-stepping algorithm. However, the stability problem is formally a (singular) boundary value problem, although the presence of the sonic point suggests that the stability determination should be independent of the upstream boundary condition. Whether the transonic solution is in fact linearly stable or possibly convectively unstable as is the case in other spatially developing flows [11] remains to be determined. In the latter case the transonic state would still appear stable since the growing perturbations would be advected downstream faster than their growth; such convectively unstable perturbations therefore decay at every fixed location. The solution of the stability problem is a challenging problem that will be considered in future work.

A related but different question concerns the temporal evolution of conditions (ρ_0, u_0) at the stellar surface that do not lie on the critical trajectory through $r = r_0$. The resulting flow must necessarily be unsteady since no spatial trajectory through $r = r_0$ with these boundary conditions satisfies the upstream boundary condition $\rho \to \rho_\infty$. Lamers and Cassinelli [16] argue that the conditions at the stellar surface, i.e., ρ_0 and hence p_0, must adjust in just such a way that the outflow speed u_0 takes the correct value provided only that the mass loss rate is sufficiently high. This adjustment process takes place via a feedback mechanism in the subsonic regime and, if correct, requires proving that the critical solution is in fact nonlinearly stable. This interesting suggestion merits further study.

Acknowledgements: PC would like to thank Nat Trask for helpful discussions. This work was supported in part by the National Science Foundation under grants DMS-1148284 (PC) and DMS-1317596 (EK), and by the Australian Research Council Future Fellowship grant FT120100309 (MW).

References

[1] W. I. Axford and R. C. Newman. Viscous-transonic flow in the accretion and stellar-wind problems. *Astrophys. J.*, 147:230–234, 1966.

[2] E. Benoit. Systèmes lents-rapides dans $\mathbb{R}^3$ et leur canards. *Astérisque*, 109–110:159–191, 1983.

[3] E. Benoit, J. Callot, F. Diener, and M. Diener. Chasse au canard. *Collectanea Mathematica*, 31:37–119, 1981.

[4] H. Bondi. On spherically symmetrical accretion. *Monthly Not. Roy. Astron. Soc.*, 112:195–204, 1952.

[5] N. Fenichel. Geometric singular perturbation theory for ordinary differential equations. *J. Diff. Eqs.*, 31(1):53–98, 1979.

[6] K. Harley, P. van Heijster, R. Marangell, G. Pettet, and M. Wechselberger. Existence of travelling wave solutions for a model of tumour invasion. *SIAM J. Appl. Dyn. Syst.*, 13:366–396, 2014.

[7] K. Harley, P. van Heijster, R. Marangell, G. Pettet, and M. Wechselberger. Novel solutions for a model of wound healing angiogenesis. *Nonlinearity*, 27:2975–3003, 2014.

[8] T. E. Holzer and W. I. Axford. The theory of stellar winds and related flows. *Annu. Rev. Astro. Astrophys.*, 8:31–60, 1970.

[9] J. M. Hong, C.-H. Hsu, and W. Liu. Viscous standing asymptotic states of isentropic compressible flows through a nozzle. *Arch. Rational Mech. Anal.*, 196:575–597, 2010.

[10] J. M. Hong, C.-C. Yen, and B.-C. Huang. Characterization of the transonic stationary solutions of the hydrodynamic escape problem. *SIAM J. Appl. Math.*, 74:1709–1741, 2014.

[11] P. Huerre and P. A. Monkewitz. Local and global instabilities in spatially developing flows. *Annu. Rev. Fluid Mech.*, 22:473–537, 1990.

[12] A. Jameson, W. Schmidt, E. Turkel, et al. Numerical solutions of the Euler equations by finite volume methods using Runge-Kutta time-stepping schemes. *AIAA*, 1259:1981, 1981.

[13] C. K. R. T. Jones. Geometric singular perturbation theory. In *Dynamical systems (Montecatini Terme, 1994)*, volume 1609 of *Lecture Notes in Math.*, pages 44–118. Springer, Berlin, 1995.

[14] C. K. R. T. Jones, T. J. Kaper, and N. Kopell. Tracking invariant manifolds up to exponentially small errors. *SIAM J. Math. Anal.*, 27:558–577, 1996.

[15] S. M. Krimigis, R. B. Decker, M. E. Hill, T. P. Armstrong, G. Gloeckler, D. C. Hamilton, L. J. Lanzerotti, and E. C. Roelof. Voyager 1 exited the solar wind at a distance of ∼85AU from the Sun. *Nature*, 426:45–48, 2003.

[16] H. J. G. L. M. Lamers and J. P. Cassinelli. *Introduction to Stellar Winds*. Cambridge University Press, 1999.

[17] L. D. Landau and E. M. Lifshitz. *Fluid Mechanics*. Pergammon Press, 1959.

[18] Y. Nie and C. Wang. Continuous subsonic-sonic flows in convergent nozzles with straight solid walls. *Nonlinearity*, 29:89–130, 2016.

[19] E. N. Parker. Parker wind. *Scholarpedia*, 3(9):7505, 2008.

[20] E.N. Parker. Dynamics of the interplanetary gas and magnetic fields. *Astrophys. J.*, 128:664–676, 1958.

[21] D. H. Rudy and J. C. Strikwerda. A nonreflecting outflow boundary condition for subsonic Navier-Stokes calculations. *J. Comp. Phys.*, 36:55–70, 1980.

[22] P. Szmolyan and M. Wechselberger. Canards in $\mathbb{R}^3$. *J. Diff. Eqs.*, 177:419–453, 2001.

[23] M. Wechselberger. À propos de canards (Apropos canards). *Trans. American Math. Soc.*, 364:3289–3309, 2012.

[24] M. Wechselberger and G. Pettet. Folds, canards and shocks in advection-reaction-diffusion models. *Nonlinearity*, 23:1949–1969, 2010.

[25] G. B. Whitham. *Linear and Nonlinear Waves.* Wiley, 1974.